DEM Response Analysis of Buried Pipelines Crossing Faults and Proposal for a Simplified Method to Estimate Allowable Fault Displacements

Yasuko Kuwata, Shiro Takada, and Radan Ivanov

Dept. of Civil Engineering, Kobe University, Japan, email: kuwata@kobe-u.ac.jp

ABSTRACT: *This paper investigates the behavior of polyvinyl chloride and ductile iron pipelines in relation to surface fault displacements using the Discrete Element Method (DEM) and proposes a method to estimate the allowable fault displacements. When modeling pipes and joints, the nonlinear material properties and joint characteristics (allowing detachment at the joints) are considered. Under a given set of various conditions with respect to pipe material, pipe diameter, crossing location and crossing angle, the allowable fault displacement to reach failure of the pipe is numerically simulated. The results show that a narrow angle between the fault line and the pipeline presents unsafe condition for the pipeline behavior. Furthermore, a simplified formula to estimate the allowable fault displacement is proposed, which considers joint failures due to axial forces. Estimated results achieved by this formula agree with the results obtained by numerical simulation. Finally, measures for installing pipelines with high performance joints are considered and discussed.*

Keywords: Discrete Element Method; Fault displacement; Buried Pipeline; Response analysis

1. Introduction

In the last decade, several destructive earthquakes created large surface fault ruptures in urban areas and caused a number of pipeline failures. To date, many active faults have been confirmed by geological research and investigations in Japan. However, many hidden active faults are believed to exist deep in the ground. Therefore, seismic countermeasures for pipeline crossing faults are urgently needed. In seismic design codes for pipelines, only the design of external loads by wave propagation and liquefaction (considered more recently) have been considered. Comprehensive knowledge of pipeline behavior under fault movement will only be obtained through further investigation.

Thus far, numerical analyses on pipeline behavior have been performed using beam or shell element models and their combined methods. Although these methods have the advantage of being simple for the simulation of rough tension behavior of pipelines under fault movement, not all of them are capable of simulating the post-detachment behavior of pipeline joints. This study uses a comprehensive numerical method developed to simulate pipeline behavior based on the Discrete Element Method (*DEM*). Here, the behavior of polyvinyl chloride (hereafter, *PVC*) and Ductile Iron Pipelines (*DIP*) is considered. Moreover, a simplified formula to estimate the allowable fault displacement is proposed, and then verified with results obtained through numerical simulation.

2. Model of Pipeline in DEM

2.1. Model of the Pipe and Soil Spring

The numerical analysis of a pipeline is performed by *DEM*, which was first developed to simulate movements of rock materials by assembling discrete elements. *DEM* can also be used for the analyses of

various materials and structures by employing new geometry for the element and spring properties. The pipeline analysis model used in this study was developed by Ivanov and Takada [1], who proposed a pipeline consisting of lumped masses and spring sets connecting them. Each spring set consists of axial, bending, and torsion components at the ends of a 3-D beam segment with Young's modulus, second moment of inertia, and length. The lumped masses are connected with two soil springs: one of them is perpendicular to the pipeline to represent the shear forces of surrounding soil, and the other is tangential to represent friction between the pipeline and soil. The contact spring is active only in compression, while the friction spring is active in both directions of the relative displacements between the pipeline and soil. At both ends of the pipeline in the model shown in Figure (1), pipe-end springs representing the spring equivalent to that of a longer pipe proposed by Liu and Takada [2], are added. The solution is based on the direct integration of uncoupled equations of motion: first, the relative displacements and rotations between each element and the other elements are calculated from a previous time step; second, the directional forces of an element originating from all other elements are summed; and third, the element positions are updated to the next time step.

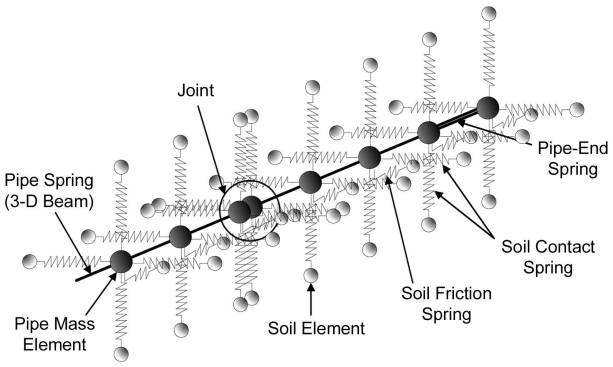

Figure 1. Model of pipeline with mass and spring.

In this model, two elements representing joints are specified at the same location, which allows disconnection of the spring when the ultimate condition of joint separation is reached. The forces and moments acting on the elements are computed according to the mechanical joint, and added to the total driving forces and moments acting on the joint. Detailed modeling of the pipe body, joint, and soil spring can be found in the papers by Morita et al [3].

2.2. PVC Pipe Model

2.2.1. Pipe Body

A *PVC* pipe with $E = 2.7\text{x}10^6\ kN/m^2$ and yield stress $\sigma_y = 1.92\text{x}10^4 kN/m^2$ is considered. Two pipes with different internal diameters (ϕ100*mm* and ϕ150*mm*) are used. The pipe of ϕ100 has diameter $d = 114mm$ and thickness $t = 7mm$, while the ϕ150 pipe has diameter $d = 165mm$ and thickness $t = 9.6mm$. When an analytical model is used, the axial forces and bending moments of *PVC* are computed separately.

PVC has good ductility under slow speed tension loading, but breaks at ultimate strain under the velocity of ground movement (around 0.5 to 1.5*m/s*). Thus, the axial spring of the pipe body is modeled as an elastic one to be cut off at the ultimate strain under tension loading. In compression loading, the axial spring is modeled to be cut off because the pipe buckles under ultimate strain. The bending spring is modeled as a nonlinear relation between the angle of rotation and the bending moment following the results of a bending test, see Figure (2).

2.2.2. Joint Property

The joint used on the *PVC* pipe is a rubber ring (*RR*) joint. The displacement and rotation behavior of this joint are shown in Figure (3), [4]. This joint has high

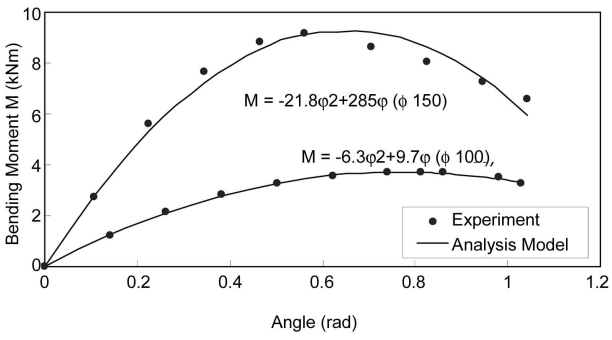

Figure 2. Pipe bending property (*PVC*).

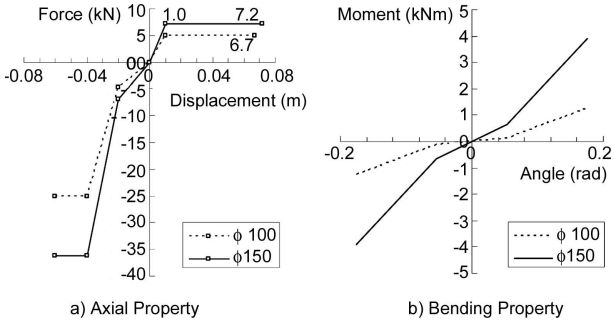

Figure 3. Rubber ring joint of *PVC*.

resistance against tension loading up to a displacement of 1.0*cm*, then sliding up to 6.7 and 7.2*cm* for ϕ100 and 150, respectively. There is no stopper to prevent detachment. On the other hand, the resistive force of the joint in compression loading is relatively high, although it is less than that of the pipe body. Compared with settlement tests of the pipeline, the proposed model of the *PVC* pipeline was confirmed by the simulation [3].

2.3. Ductile Iron Pipe Model

2.3.1. Pipe Body

For the *DIP*, Young's modulus $E = 1.6 \times 10^8 kN/m^2$ and yield stress $\sigma_y = 4.2 \times 10^5 kN/m$ are considered [5]. Two pipe diameters (ϕ100 and ϕ150) are used. The pipe with ϕ100 has diameter $d = 118mm$ and thickness $t = 6mm$, while the ϕ150 pipe has diameter $d = 169mm$ and thickness $t = 6mm$. As with the *PVC* pipe, the axial forces and bending moments of *DIP* are computed separately based on the pipe experiments [4]. The properties of the pipe body under axial force are modeled by the linear behavior up to the ultimate strain, and the properties of the bending moments are considered by elastic-plastic methods, as shown in Figure (4), [5].

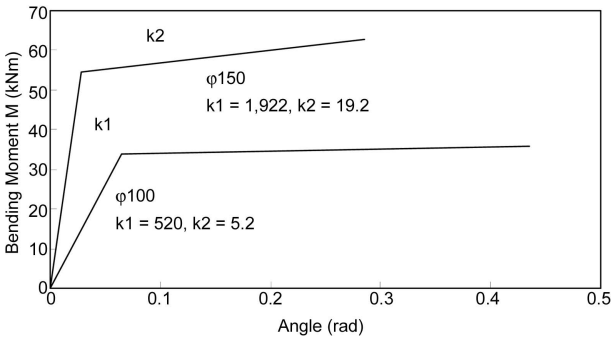

Figure 4. Pipe bending property (*DIP*).

2.3.2. Joint

A *GM-II* joint (gas mechanical joint) is used in the analysis, as shown in Figure (5), [6]. This joint features a unique ring to reduce compression forces.

3. Case Studies of Pipe Behavior of *PVC* and *DIP*

3.1. Analysis Model

The model consists of five 5*m* pipe segments interconnected by four joints, with Joints *A* to *D* being placed consecutively from the left-hand side, as shown in Figure (6). The fault intersects the pipeline

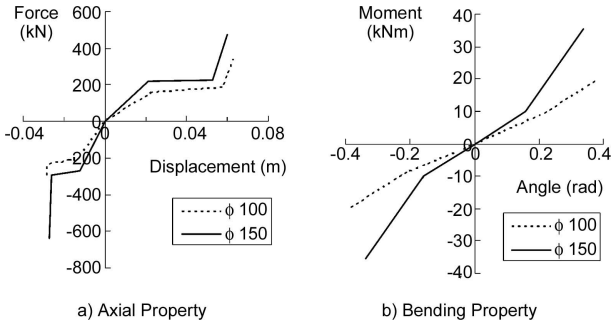

Figure 5. *DIP* Gas mechanical anti-seismic joint.

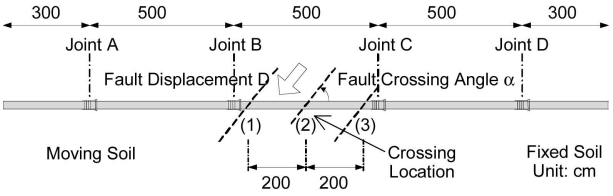

Figure 6. Analysis model.

at three locations between Joints *B* and *C*, with the crossing angle α varying between 30 and 150 degrees. Cases with a crossing angle of less than 90 degree correspond to normal fault movements, giving rise to tension forces on the pipeline, while cases with a crossing angle of greater than 90 degrees correspond to reverse faults with compression forces. The fault displacement is applied upwards on the left-hand side of the model. With regard to interactions between the soil and the pipe, soil spring activity between relative displacements and forces are modeled by an elastic-plastic body based on the seismic design guidelines published by the Japan Gas Association [7]. The contact soil spring representing shear force of the soil is modeled similarly based on this guideline as a firm ground condition. The stiffness of the soil spring on the left-hand side of the model is one third of that on the right-hand side, and is based upon the experimental data acquired thus far [8]. Although the numerical analysis is capable to be given forces in three dimensions, the analysis model herein uses external displacements in vertical and one horizontal.

3.2. Results

In the analysis model, the pipeline has compression forces on the side where there is soil movement and tensile forces on the side where the soil is static. Bending moment distributions of *PVC* and *DIP* pipelines are shown in Figure (7). The bending moment of the *PVC* pipeline occurs only in a single

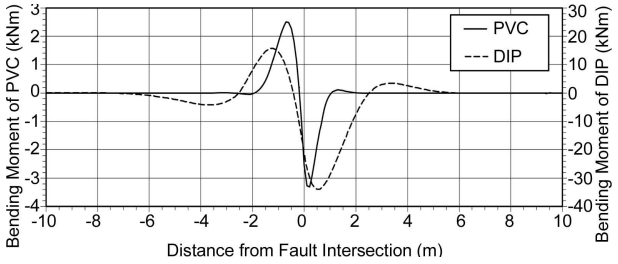

Figure 7. Bending moment of pipeline.

pipe segment (plus or minus 2.5*m* from the fault intersection), while in the case of *DIP*, the bending moment is transferred to the adjacent pipe segments because of the high rigidity of the pipe body. Therefore, the bending moment of a *DIP* is much larger than that of a *PVC* pipe.

An allowable fault displacement is determined under the conditions that the joint exhibits either the behavior of pulling out or its material yields under compression, or that the pipe body reaches its yield strength. The results of numerical computation show different displacements according to the fault crossing angle as shown in Figure (8). Both the *PVC* and *DIP* pipelines show similar trends for allowable fault displacements, especially where the crossing angle of 90 degree results in greater displacement values.

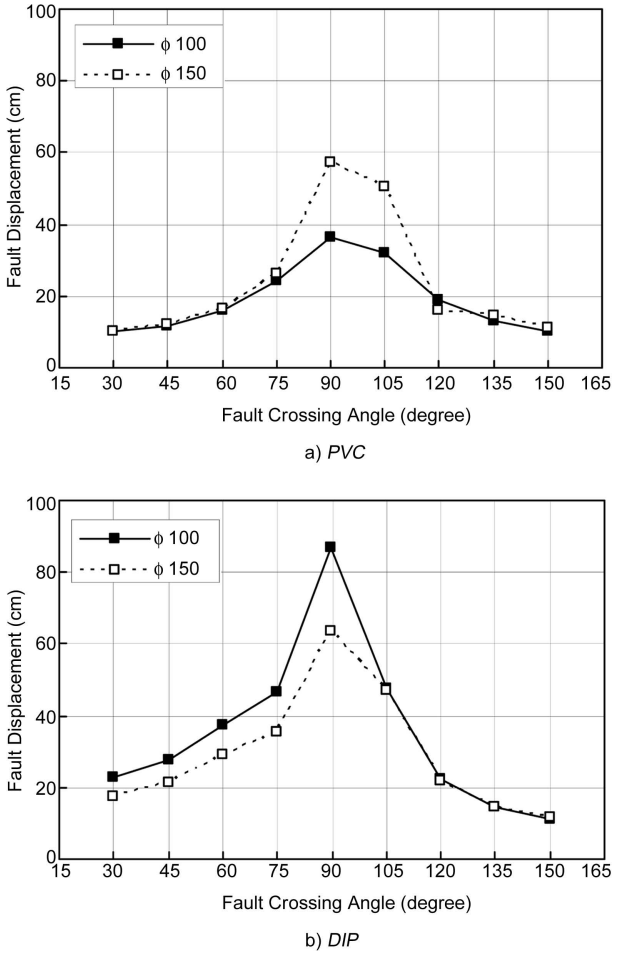

Figure 8. Allowable fault displacement vs. fault crossing angle.

With regard to the failure mode and location, in cases with a crossing angle of less than 60 degrees, the Joint B in crossing locations (1) and (2) and Joint *C* in crossing location (3) are pulled out of place, thus breaking the connection. In cases with a crossing angle greater than 120 degrees, the joints are broken by compression rupture (the relationship between joint failure and the fault crossing location are similar to the cases with tension forces). However, it is observed that, throughout the given range of these crossing angles, the failure clearly occurs at the joint. In the range of angles between 75 and 105 degrees, the bending moment is stronger than the axial force; therefore, the bending failure occurs on either the pipe body or the joint. In the other parametric analyses considering soil stiffness, the allowable fault displacement in that range of angles varies by the shear performances of soil, but there are few effects on those in the range of angles of less than 60 degrees or greater than 120 degrees [3].

4. Proposal for a Simplified Formula to Estimate Allowable Fault Displacements

4.1. Concept

Here, it is assumed that a single fault line intersects a pipeline, and the proposed formula focuses on cases where the fault crossing angle is less or greater than 90 degrees. As the angle increases or decreases from 90 degrees, the allowable fault displacement becomes smaller and axial forces cause joints to fail. It is noted that the effects of bending moments become larger caused by shear force of surrounding ground when the fault crossing angle is close to 90 degrees. In the range of angles of less than 60 degrees or greater than 120 degrees, the shear performance of the soil does not strongly affect on the results. The estimation of allowable fault displacements based on axial forces is considered to be safe practice. However, fault movements with crossing angles of 90 degrees, causing mostly bending failures on pipes with few axial forces, do not follow the estimation concept.

Pipelines are easily ruptured with joints becoming detached when the ground surface becomes largely deformed by normal or reverse faulting. Among these failure modes, as both the pipeline and fault line have narrow angles, the geometry of the pipeline and its relationship with the fault displacements are the

dominant factors causing joint failures. In other words, pipeline behavior can be explained only by the displacement characteristics concerning the tension and compression of pipes and joints on which axial forces act, see Figure (9). The following 4 points explain the concept of joint failure mechanisms using the fault crossing angle α.

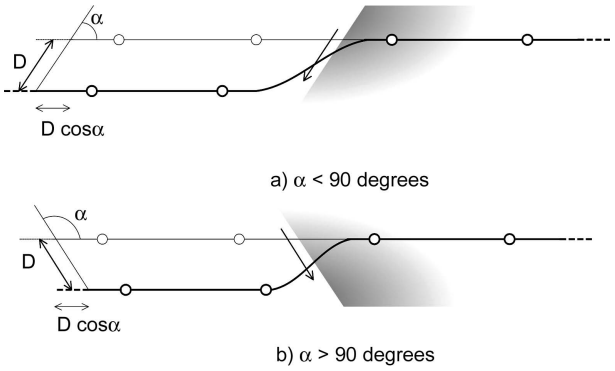

Figure 9. Geometry at joint failure.

1. In the cases where α = 0 or 180 degrees, the fault displacement activities at the time of pipe detachment or rupture can be pipe displacement D_0 or D_{180}. When α<90 degrees, the allowable fault displacement is close to the fault displacement D_0 multiplied by the inverse of *cos*α. On the other hand, when α>90 degrees, the allowable fault displacement is close to the fault displacement D_{180}, multiplied by the inverse of *cos*α. However, if the fault crossing angle is 90 degrees, or close to it, the concept based on axial force is not suitable for estimation because the bending moment dominates pipeline behavior.
2. Under fault displacement, soil friction forces on pipelines have a peak value at the fault crossing location. Although the soil spring with large deformations between the pipe and soil is in plastic state, when maximum friction coefficient constants are considered (in numerical analyses, the relative displacement between pipe and soil is 0.5*cm* at yield point), the axial force decreases proportionally in terms of the soil friction force according to the length from the peak location.
3. Location of the joint failure is determined by the maximum axial forces acting upon sliding and static soils, as well as the distance of the joint from the fault. Moreover, axial forces acting on the pipeline at the time of failure are the same as the maximum resistive forces of the joint.
4. With regard to the distribution of soil friction forces in the longitudinal direction of the pipeline, the displacements on the joint and pipe are calculated. In case of fault crossing angle α, the summation of the displacements of both pipe and joint multiplied by the inverse of *cos*α could estimate the allowable fault displacement.

4.2. Calculation Method

As an example, allowable fault displacements can be calculated using schematic figures and equations. Figure (10) shows the distribution of axial forces on pipelines in the case where the fault crossing angle is 0 degree.

In Figure (10), the maximum soil friction force per unit length on the left-hand side of the model is *f* (*kN/m*), and that on the right-hand side is *cf* (*kN/m*). Joints on the left-hand side are J_{L1}, J_{L2}, …, J_{Ln} from the fault, and those on the right-hand side are J_{R1}, J_{R2}, …, J_{Rn}, where the axial force at joint J_i is F_i, and the amount of displacement is δ_i. The intersected pipe segment is named as P_c, and the another pipe segment between joints J_i and J_{i+1} is named as P_i. The single pipe length is *l* (*m*) and the length from joint J_{L1} to the fault crossing location is *x*.

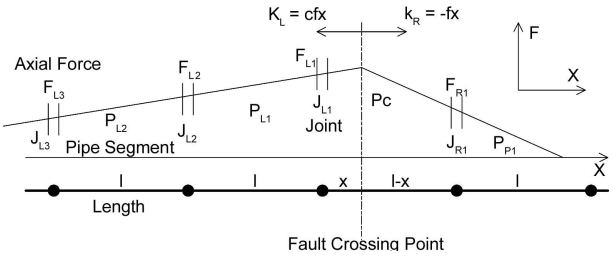

Figure 10. Distribution model of axial soil friction forces.

In the case of $0 \le x \le 1/(c+1)l$, joint J_{L1} has a detachment failure when α< 90 degrees, or a compression rupture when α > 90 degrees. The axial force at joint J_{L1} reaches the ultimate resistive force of the joint, F_{max}, and the axial forces on the other joints are determined according to F_{max} at joint J_{L1}, following the arithmetical progression of soil friction forces. Furthermore, the number of joints having effective displacements, n_L and n_R on the left- and right-hand sides, respectively, are also calculated. Axial forces at joints on the left-hand side can be calculated by

$$F_{Ln} = F_{max} - \gamma_\alpha c f l(n-1), \qquad (1)$$

where, $n = 1, \cdots, n_L (= Int(F_{L1}/cfl)+1)$, and the symbol of *Int*(*x*) is the integral value of *x*; if α< 90 degrees,

$\gamma_\alpha = 1$, otherwise $\gamma_\alpha = -1$.

Similarly, the axial forces on joints on the right-hand side are given by

$$F_{Rn} = F_{max} + \gamma_\alpha (c+1) f x - \gamma_\alpha n f l, \quad (2)$$

where, $n = 1, \cdots, n_R (= Int(F_{R1} / f l) + 1)$; if $\alpha < 90$ degrees, $\gamma_\alpha = 1$, otherwise $\gamma_\alpha = -1$.

When the relationship between the displacements and axial forces on a joint is given by $F = g(\delta)$, the summation of the joint displacements at the time of failure δ_P can be expressed by

$$\delta_J = \sum_{n_L} \delta_{Li} + \sum_{n_R} \delta_{Ri} = \sum_{n_L} g'(F_{Li}) + \sum_{n_L} g'(F_{Ri}) \quad (3)$$

in which $g'(x)$ is the inverse of function $g(x)$.

At the same time, the displacement of the pipe body, δ_P, is the summation of the displacements at the intersected pipe segment P_c and the effective pipe segments of n_L - 1 and n_R - 1 expressed with Young's modulus E and section area of pipe A as

$$\delta_P = \frac{\gamma_\alpha f}{2EA} \left\{ c(n_L l + x)^2 + ((n_R + 1) l - x)^2 \right\} \quad (4)$$

This formula does not consider the displacement of other pipe segments that are located further away from the effective pipes that have larger friction forces. Otherwise, there is the need to solve complicated equations, including soil friction variables. Finally, the allowable fault displacements can be estimated using the total displacement of joints and pipes and fault crossing angles by

$$D = (\delta_J + \delta_P) / cos\alpha \quad (5)$$

On the other hand, in the case of $1/(c+1)l \le x \le l$, joint J_{R1} has a detachment failure when $\alpha < 90$ degrees or a compression rupture when $\alpha > 90$ degrees. Similar to the case of $0 \le x \le 1/(c+1)l$, the axial force at the joint is determined according to F_{max} at joint J_{R1} on the right-hand side as follows:

$$F_{Rn} = F_{max} - \gamma_\alpha f l (n-1) \quad (6)$$

where, $n = 1, ..., n_R (= Int(F_{R1} / f l) + 1)$; if $\alpha < 90$ degrees, $\gamma_\alpha = 1$, otherwise $\gamma_\alpha = -1$. On the left-hand side

$$F_{Ln} = F_{\max} + \gamma_\alpha (1+c) f x - \gamma_\alpha n f l \quad (7)$$

where, $n = 1, ..., n_L (= Int(F_{L1} / cf l) + 1)$; if $\alpha < 90$ degrees, $\gamma_\alpha = 1$, otherwise $\gamma_\alpha = -1$.

The following calculations of allowable fault displacement can be done by Eq. (3-5), and the case of $0 \le x \le 1/(c+1)l$.

4.3. Comparisons

Compared with the allowable fault displacements computed by *DEM* response analysis, the fault displacements obtained by the proposed estimation method correlate well. Figure (11) shows the fault displacement results of the numerical analysis and the proposed estimation method for both the *PVC* and *DIP* pipes. The estimated figures show good agreement, especially with fault crossing angles of less than 60 degrees for detachment failures and more than 135 degrees for compression ruptures. Around 90 degrees, the estimation figures separate from those of the *DEM* analysis since bending moments are the predominant cause of pipe failures.

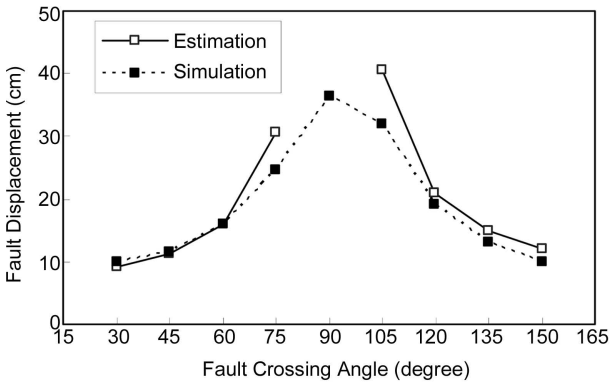

a) *PVC*

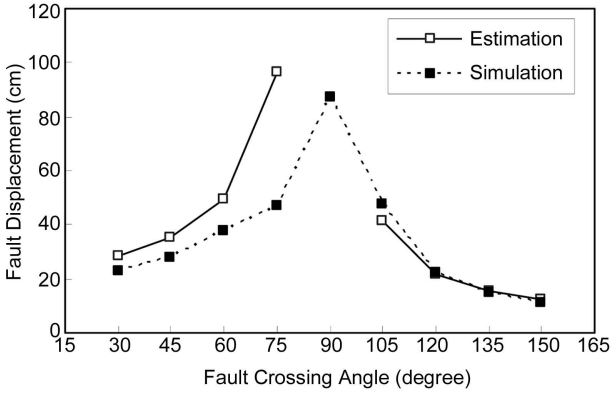

b) *DIP*

Figure 11. Allowable fault displacements of estimation and numerical analysis.

Although the *DEM* numerical analysis for *DIP* pipelines was modeled using three pipe segments, the simplified estimation method shows higher number of effective pipes in comparison with the *DEM* numerical results. Longer pipelines and the interaction between the soil and joint in the *DEM* numerical model need to be considered.

5. Countermeasures

In this section, the behavior of a *PVC* joint is considered as a seismic countermeasure. Apart from the original joint, type *RR* shown in Figure (3), the axial properties under tension and bending moments of another joint, long rubber ring (*LRR*) type, are modeled as shown in Figure (12). The *LRR* joint features large allowances in both axis and rotation due to the incorporation of stopper and longer connections. The axial properties under compression are the same as the original because stiffer joints under compression cause buckling failures on pipes and cannot be calibrated using the simplified estimation method.

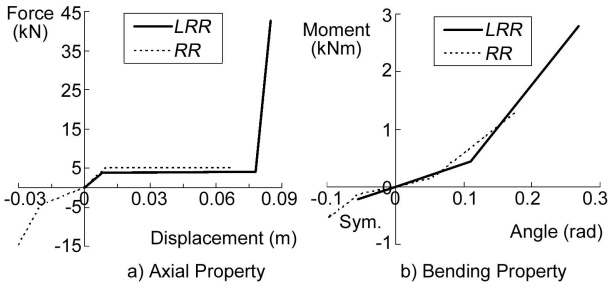

Figure 12. Joint model of *PVC*.

The allowable fault displacements of *LRR* joints obtained by the *DEM* numerical simulation are much longer than those of *RR* joints because the stopper improves pipeline performance, as shown in Figure (13). With a crossing angle of over 75 degrees, the pipe was simulated to its bending failure, even though the joint was stronger. Therefore, it can be concluded that high performance joints are effective for with standing fault displacements in cases where there is a crossing angle of less than 60 degrees.

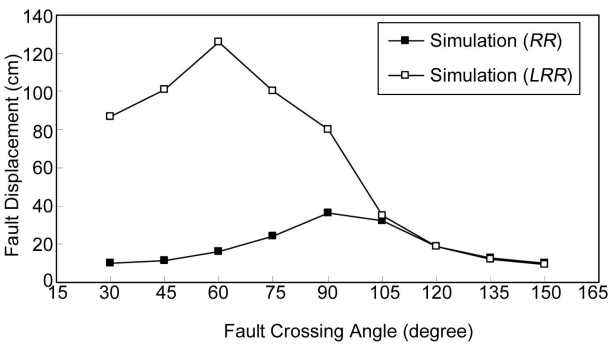

Figure 13. Performances of *RR* and *LRR*.

In practice, for seismic countermeasures, not only strong pipe property (pipe body and joint) but also other ways such as construction method and redundancy of network could contribute to mitigating direct and indirect damages.

6. Conclusions

A *DEM* numerical simulation of a pipeline under fault displacement conditions and a simplified method for estimating allowable fault displacements are presented.

Pipelines modeled by *DEM* showed behavioral characteristics of the pipeline, such as detachment of joints with normal fault movements, compression rupture of joints in reverse fault movements, and bending failure at either joints or the pipe body under a crossing angle of 90 degrees.

The proposed simplified estimation method compares well for cases where the fault crossing angle is less than 60 degrees or greater than 120 degrees. By neglecting bending moments, the simplified method could not estimate the allowable fault displacements well compared to those by the *DEM* method in cases where the crossing angle was approximately 90 degrees. However, for safe practice, this estimation method could be useful.

Both the *DEM* numerical simulation and the simplified estimation method have shown that a high performance joint can effectively decrease bending failures on pipelines.

References

1. Ivanov, R. and Takada, S. (2003). "Numerical Simulation of the Behaviour of Buried Jointed Pipelines under Extremely Large Fault Displacements", *TCLEE*, *ASCE*, 717-726.

2. Liu, A. and Takada, S. (2002). "Study on the Performances of Two Large-Diameter Steel Pipelines at Fault Crossing in Kocaeli and Ji-Ji Earthquake", *Proc. of the Fourth China-Japan-USA Trilateral Symposium on Lifeline Earthquake Engineering*, China, 153-160.

3. Morita, N., Kuwata, Y., and Takada, S. (2004). "Analysis on Behavior of Polyvinyl Chloride Pipeline Crossing Faults Considering Nonlinear Material Property by Discrete Element Method", Memoirs of Construction Engineering Research Institute, 46B, 127-139, Japan.

4. Takada, S., Hazama, Y., Ito, T., Ueno, T., Yamajo, K., and Irioka, T. (1985). "Development of Manhole Fitting Unplasticized Polyvinyl Chloride Pipeline System Resisting Ground Subsidence", *Proc. of Pressure Vess. and Piping Conference (ASME)*, **98**(4), 55-60.

5. Kubota, Co. ltd. (1978). "Ductile Pipe Handbook", Osaka, Japan.

6. Takada, S. (1984). "Model Analysis and Experimental Study on Mechanical Behaviour of Buried Ductile Iron Pipelines Subjected to Large Ground Deformation", *The 8th World Conf. on Earthquake Engineering (8WCEE)*, **8**, 263-270.

7. Japan Gas Association (1982). "Recommended Standards for Earthquake Resistant Design of Gas Pipelines", *JGA*, Tokyo, Japan.

8. Takada, S., Nakano, M., Katagiri, S., Tani, K., and Koyanagi, S. (1999). "Experimental Study on Earthquake-Proof U-PVC Pipeline Subjected to Uneven Ground Settlement During Earthquakes", *J. of Japan Society of Civil Engineers*, 619, I-47, 145-154.